

段士刚, 张作衡, 魏梦元, 等. 新疆西天山雾岭铁矿闪长岩地球化学及锆石 U-Pb 年代学[J]. 中国地质, 2014, 41(6): 1757-1770.  
Duan Shigang, Zhang Zuoheng, Wei Mengyuan, et al. Geochemistry and zircon U-Pb geochronology of the diorite associated with the Wuling iron deposit in Western Tianshan Mountains, Xinjiang[J]. Geology in China, 2014, 41(6): 1757-1770(in Chinese with English abstract).

# 新疆西天山雾岭铁矿闪长岩地球化学 及锆石 U-Pb 年代学

段士刚<sup>1,2</sup> 张作衡<sup>2</sup> 魏梦元<sup>3</sup> 田敬俊<sup>3</sup> 蒋宗胜<sup>2</sup> 李凤鸣<sup>4</sup> 赵军<sup>1</sup> 王厚方<sup>3</sup>

(1. 长安大学 地球科学与资源学院, 陕西 西安 710054; 2. 中国地质科学院矿产资源研究所 国土资源部成矿作用与资源评价重点实验室, 北京 100037; 3. 新疆地矿局第三地质大队, 新疆 库尔勒 841000; 4. 新疆维吾尔自治区地质矿产勘查开发局, 新疆 乌鲁木齐 830000)

**提要:** 雾岭闪长岩呈单式岩株状侵入于石炭系大哈拉军山组火山碎屑岩中, 在闪长岩内部和接触带发现了铁矿体。闪长岩锆石 U-Pb 年龄为  $(307.7 \pm 0.8)$  Ma, 于晚石炭世侵位。岩石具有正的  $\varepsilon_{\text{Nd}}(t)$  值 (3.1~4.6) 和相对低的初始  $^{87}\text{Sr}/^{86}\text{Sr}$  比值 ( $0.7043 \sim 0.7046$ ), Nd 模式年龄为  $695 \sim 818$  Ma, 在  $^{87}\text{Sr}/^{86}\text{Sr}(t) - \varepsilon_{\text{Nd}}(t)$  图解上位于地幔趋势线上, 表明地幔是闪长岩的源区, 但 Th 含量 ( $1.61 \sim 3.24 \mu\text{g/g}$ ) 和 Th/Ta 比值 (6.1~7.9) 较高, 指示受到了陆壳混染作用的影响。因此认为, 该岩浆可能是由玄武质岩浆与地壳物质相互作用而发生分离结晶作用后形成。通过综合分析认为, 雾岭闪长岩虽然保留有岛弧岩浆作用的痕迹, 但其实是板内环境的产物, 是在西天山增生造山结束、伊犁微陆块与塔里木板块发生块体间旋转时侵位的, 其成因可能与伊犁微陆块内造山带根部拆沉作用或局部形成的挤压-伸展的构造转变带有关。

**关 键 词:** 海相火山岩型铁矿; 锆石 U-Pb 年龄; Sr、Nd 同位素; 雾岭; 阿吾拉勒; 西天山

**中图分类号:** P588.12<sup>2</sup>; P597    **文献标志码:** A    **文章编号:** 1000-3657(2014)06-1757-14

中亚造山带是典型的增生型造山带和全球显生宙大陆地壳生长最显著的地区<sup>[1-3]</sup>, 也是研究增生造山成矿作用的理想区域<sup>[4-5]</sup>。海相火山岩型铁矿是中亚造山带特色成矿类型之一, 广泛分布于哈萨克斯坦的图尔盖洼地、阿尔泰和天山地区<sup>[6-8]</sup>。中国天山造山带内铁矿资源丰富, 海相火山岩型铁矿储量大、富矿多、富矿比例高、矿化特征显著, 是探索增生造山过程中海相火山岩型铁矿成矿作用的优秀选区。近年来, 天山造山带海相火山岩型铁矿勘查工作又取得重大进展, 于新疆西天山阿吾拉勒成

矿带内相继勘查或发现了查岗诺尔、备战、智博和敦德 4 个大型铁矿, 松湖、尼新塔格—阿克萨依、铁木里克、苏洛、沙拉穹库尔及雾岭等多个中-小型铁矿床或矿点, 使阿吾拉勒铁矿带新增成为新疆重要的大型铁矿开发基地<sup>[9]</sup>。西天山阿吾拉勒成矿带内海相火山岩型铁矿在晚石炭世成矿<sup>[9-11]</sup>。近年来蛇绿岩、高压变质岩和花岗岩类等的大量研究数据表明, 西天山在早石炭世末结束增生造山, 二叠纪进入后碰撞演化阶段<sup>[12]</sup>, 在晚石炭世经历了由汇聚到伸展的转变<sup>[13-14]</sup>。晚石炭世特殊的大陆动力学背

收稿日期: 2014-09-30; 改回日期: 2014-10-10

基金项目: 国家科技支撑计划(2011BAB06B02)、国家自然科学基金项目(41203035)、国家重点基础研究发展计划(2012CB416803)

和中国地质调查局地质矿产调查评价项目(1212011090300)联合资助。

作者简介: 段士刚, 男, 1983 年生, 博士, 助理研究员, 研究方向为矿床学与矿床地球化学; E-mail: dsg1102231@163.com。

景是区内海相火山岩型铁矿形成的前提。本文着重研究该地区晚石炭世雾岭闪长岩体产生的大地构造环境和岩浆作用性质,为探索西天山海相火山岩型铁矿的成矿地质背景提供重要约束。

## 1 区域地质背景

雾岭铁矿化岩体所在的阿吾拉勒山呈东西向横亘于西天山伊犁微陆块之内(图1)。伊犁微陆块具有太古宇和古元古界结晶基底<sup>[15]</sup>,可能由罗迪尼亞超大陆裂解而来<sup>[16]</sup>。晚古生代早期,伊犁微陆块南北分别为南天山洋和北天山洋所俯冲<sup>[17~18]</sup>。南天山洋在泥盆纪末至早石炭世末期间逐渐闭合,塔里木板块与伊犁微陆块发生碰撞,并在二叠纪之前完成碰撞<sup>[17, 19~20]</sup>,在早二叠世两者已联为一个整体<sup>[21~22]</sup>。北天山洋在晚石炭世末闭合,从早二叠世开始整个西天山地区进入后碰撞演化阶段<sup>[17, 23~26]</sup>。

区域上出露的岩石地层有:中元古界星星峡群基底变质岩石,主要为大理岩、黑云母斜长片麻岩和角闪二长片麻岩;志留系主要为一套碳酸盐岩-火山岩建造;中泥盆统,为一套海相火山碎屑岩建造夹少量正常碎屑沉积岩,上泥盆统,为一套滨海-海陆交替相火山岩、陆源碎屑岩和碳酸盐岩建造;

石炭系为区内铁矿围岩,分布最广泛,被划分为大哈拉军山组的一套海相火山喷发-沉积碎屑岩夹碳酸盐岩建造,和上石炭统伊什基里克组的一套局部夹正常沉积岩和灰岩的火山角砾岩、凝灰岩和熔岩;下二叠统,一套正常陆源碎屑沉积岩;下一中三叠统,一套紫红色陆源碎屑岩;侏罗系,主要为砾岩、砂岩夹炭质泥岩及煤层<sup>[27~30]</sup>。

阿吾拉勒铁矿带铁矿床的围岩火山-火山碎屑岩被统一归入大哈拉军山组。但是,最新的一系列锆石 SHRIMP、LA-ICP-MS 高精度年代学研究均表明,“大哈拉军山组”火山岩并非同一期岩浆活动的产物,可能包括了中泥盆世—晚石炭世的一系列火山岩<sup>[31~36]</sup>,将来可能会被解体<sup>[33]</sup>。

阿吾拉勒山断裂构造十分发育,最明显的断裂是呈北西西走向的大断裂及其两侧发育的一系列近于平行的断裂,共同构成了近东西向或北西西向的断裂带。此外北东向和北西向断裂在区内分布也十分广泛,它们往往错断北西西向的大断裂,形成菱形的构造格局<sup>[37]</sup>。与区域主要构造形迹相关,阿吾拉勒山的褶皱构造轴迹方向亦为近东西向,规模较大的褶皱以开阔褶皱为主,规模较小的以同斜褶皱为特征<sup>[30]</sup>。

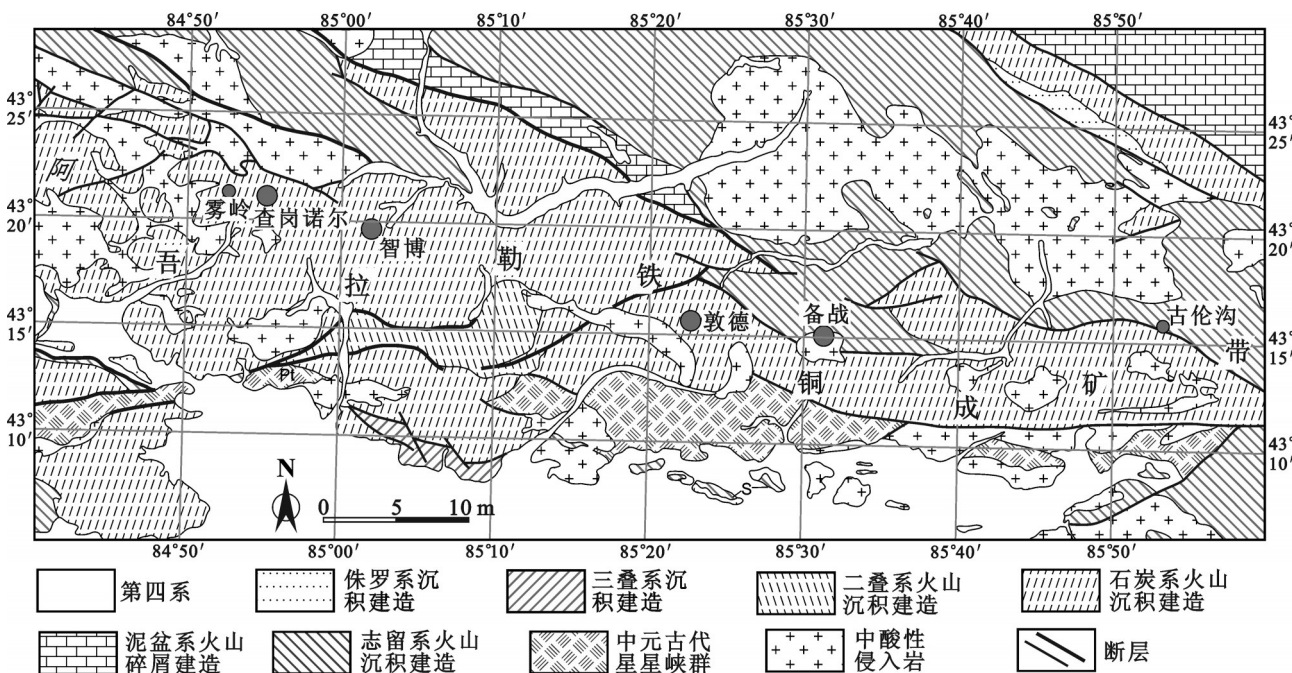


图1 新疆西天山阿吾拉勒铁铜成矿带东段地质图(修改自文献[5])

Fig.1 Geological map of the eastern segment of the Awulale iron-copper metallogenic belt in Western Tianshan, Xinjiang  
(after reference [5])

阿吾拉勒山侵入岩比较发育,空间上以中部(查岗诺尔铁矿及以西地区)分布最为广泛,向东西两侧减弱;时代上从东向西由泥盆纪为主,到石炭纪为主,再到二叠纪侵入岩为主。东部主要为泥盆纪石英闪长岩,石炭纪花岗岩、花岗闪长岩、闪长岩及石英闪长岩,二叠纪花岗岩等;中部主要为大面积的二叠纪花岗岩、闪长岩和石英闪长岩,少量二长花岗岩、正长花岗岩,及少量石炭纪闪长岩、花岗闪长岩<sup>[36, 38-40]</sup>;西部主要为二叠纪花岗斑岩、闪长岩、闪长岩和少量辉绿岩、埃达克质钠长斑岩<sup>[41]</sup>。

## 2 雾岭闪长岩地质和岩石学特征

雾岭闪长岩体位于查岗诺尔铁矿西侧约8 km(图1)。岩体呈单式岩株状侵入于石炭系大哈拉军山组火山碎屑岩中,围岩岩性主要为晶屑凝灰岩、凝灰岩、凝灰砂岩,夹少量基性-酸性熔岩及碳酸盐岩<sup>[30]</sup>(图2,图3-a)。1:5万航磁调查显示,有一个强磁异常对应于雾岭闪长岩体的东南部,异常曲线尖锐,强度高(991nT),指示雾岭岩体的铁矿找矿前景良好<sup>[30]</sup>。目前于岩体内发现一条磁铁矿体(为矿区主要矿体),在岩体接触带发现2条小型磁铁矿体,

另外在岩体内和接触带发现多处磁铁矿化,矿化均伴随有钠长石化、透辉石、绿帘石化等蚀变,一般以绿帘石化蚀变为主。岩体内发现的磁铁矿体,长约50 m,宽约20 m(图3-b),产状 $195^{\circ}\angle 62^{\circ}$ ,围岩为灰绿色绿帘石化中一细粒闪长岩,金属矿物主要为磁铁矿、黄铁矿,矿石结构较单一,他形一半自形细一中粒结构,块状构造、浸染状构造,全铁品位27.17%~58.64%,平均44.98%,矿体被早二叠世辉绿玢岩穿切(图2)。矿体周围蚀变以钠长石化、绿帘石化为主。钠长石化强烈地段形成了完全由钠长石组成的白色钠长石岩,及粗晶钠长石-绿帘石脉(图3-e,3-f),远离矿体的地段蚀变很弱。

闪长岩为灰白色,半自形-自形粒状结构,块状构造,镜下观察可知主要矿物为斜长石(含量60%左右)、角闪石(25%)、石英(5%)、单斜辉石(<5%),副矿物有锆石、磁铁矿、钛铁矿、榍石和磷灰石等(图3-g-i)。斜长石自形板条状,自形程度较高,环带结构发育,以中长石为主。角闪石为普通角闪石,呈自形长柱状,浅棕色-绿褐色多色性,解理发育。单斜辉石细粒状,边部多被溶蚀。石英呈他形粒状,星散状、填隙状分布。在QAP三角图解中主

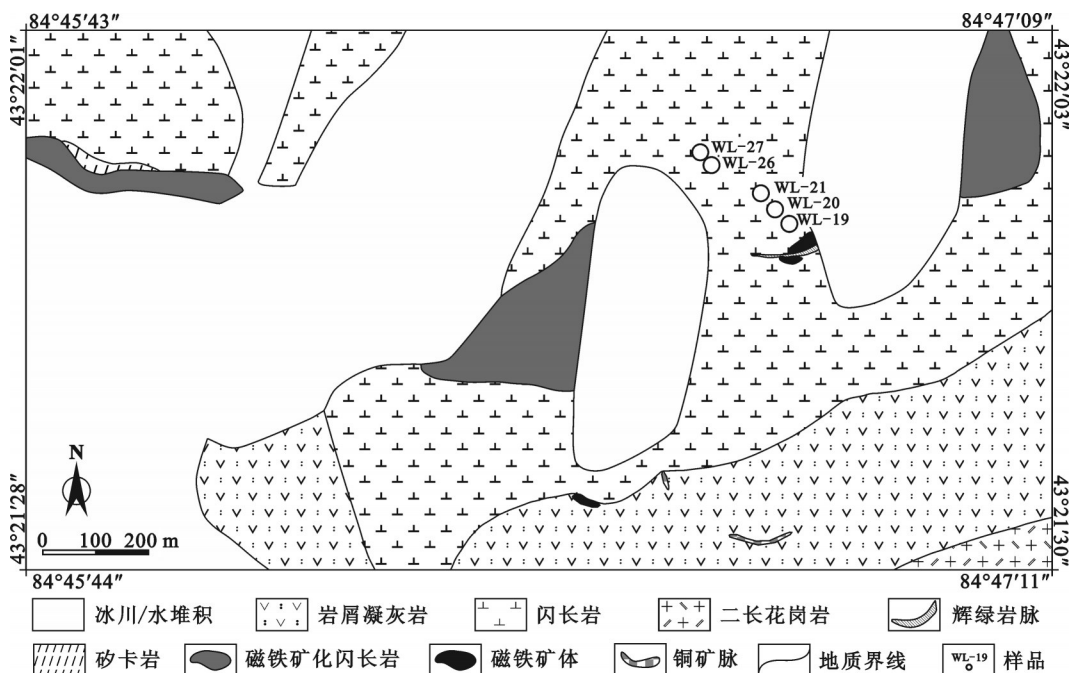


图2 新疆西天山雾岭岩体地质简图  
Fig.2 Geological sketch map of the Wuling diorite intrusion

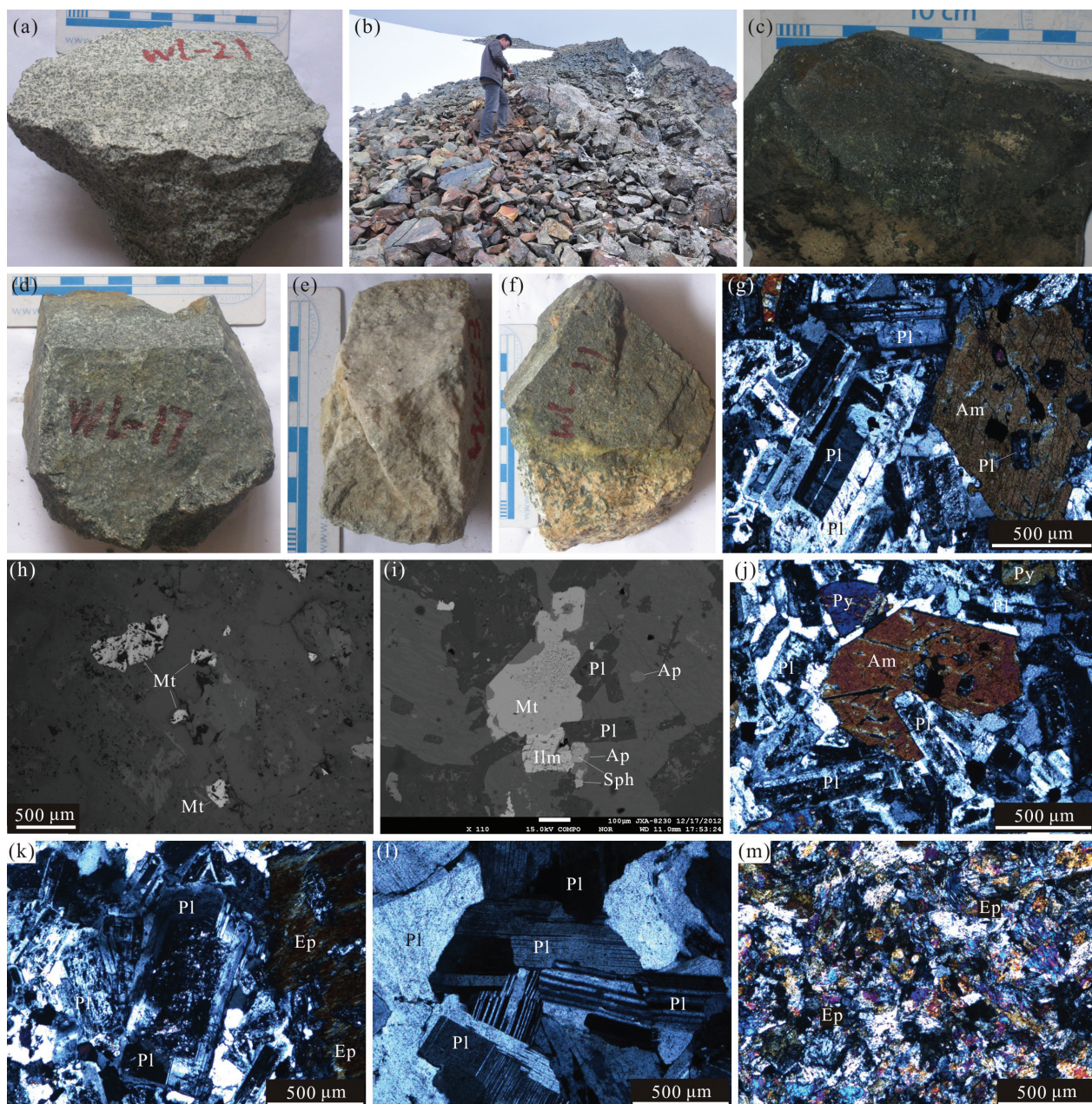


图3 新疆西天山雾岭岩体闪长岩典型照片

a—新鲜闪长岩样品；b—闪长岩体中铁矿露头；c—磁铁矿石；d—磁铁矿—绿帘石化闪长岩；e—闪长岩体中铁矿体附近的钠长石脉；f—磁铁矿化闪长岩中的粗晶钠长石—绿帘石脉；g—角闪石边部受斜长石交代(透射正交偏光)；h—闪长岩中的磁铁矿(反射单偏光)；i—闪长岩中的磁铁矿、钛铁矿、闪锌矿和磷灰石(反射单偏光)；j—闪长岩中残留的他形辉石(透射正交偏光)；k—绿帘石化、钠长石化蚀变闪长岩长石发育斜长石净边(透射正交偏光)；l—钠长石脉(透射正交偏光)；m—绿帘石蚀变(透射正交偏光)；Am—角闪石；Ap—磷灰石；Ep—绿帘石；Mt—磁铁矿；Pl—斜长石；Py—辉石；Sph—闪锌矿

Fig.3 Representative photographs of the Wuling magnetite mineralized diorite

a—Fresh diorite sample; b—Iron orebody outcrops within diorite; c—Magnetite ore; d—Magnetite and epidotized diorite; e—Albite veins in the vicinity of iron orebody within diorite; f—Coarse grained albite-epidote veins in magnetitized diorite; g—Hornblende replaced by plagioclase (transmission crossed nicols); h—Magnetite in diorite (reflection plainlight); i—Magnetite, ilmenite, sphalerite and apatite in diorite (reflection plainlight); j—Residue of anhedral pyroxene in diorite (transmission crossed nicols); k—Net edge of plagioclase in epidotized and albitized diorite (transmission crossed nicols); l—Albite veins (transmission crossed nicols); m—Epidote alteration (transmission crossed nicols); Am—Amphibole; Ap—Apatite; Ep—Epidote; Mt—Magnetite; Pl—Plagioclase; Py—Pyroxene; Sph—Sphalerite

要投影于闪长岩和石英闪长岩分界线附近。

### 3 测试方法与测试结果

#### 3.1 样品采集与实验方法

样品采自闪长岩体内部,从距离铁矿体约30 m 蚀变很弱的地段开始,由WL-19到WL-27逐步远离矿体,样品间隔20 m至50 m不等。火成岩样品的主量、微量元素和稀土元素分析在中国地质科学院国家地质测试中心完成。先将样品无污染粉碎至200 目,然后主量元素 $\text{SiO}_2$ 、 $\text{Al}_2\text{O}_3$ 、 $\text{TiFe}_2\text{O}_3$ 、 $\text{Na}_2\text{O}$ 、 $\text{K}_2\text{O}$ 、 $\text{CaO}$ 、 $\text{MgO}$ 、 $\text{TiO}_2$ 、 $\text{MnO}$ 、 $\text{P}_2\text{O}_5$ 等采用荧光光谱(XRF)法在X荧光光谱仪(3080E)上测试,FeO采用滴定法分析, $\text{CO}_2$ 含量采用硫酸汞溶液加热释气法, $\text{H}_2\text{O}^+$ 采用双球管灼烧冷凝水称重法,LOI为高温加热后重量和灼烧后重量之差。微量元素和稀土元素组成采用电感耦合等离子体质谱(ICP-MS)法在离子质谱仪(X-series)上测试。

锆石U-Pb同位素测年在中国地质科学院矿产资源研究所LA-ICP-MS实验室完成。样品经破碎后,采用常规重力和磁选方法分选出锆石,用环氧树脂制作成样品靶,经抛光后,对锆石进行阴极发光(CL)、透射光和反射光等显微照相,观察和对比锆石内部结构、包裹体、裂隙等特征,选取适宜的测试点位进行测试。测定之前用酒精轻擦样品表面,以除去可能的污染。测试所用仪器为连接New-Wave UP-213激光剥蚀系统的Finnigan Neptune型MC-ICP-MS。仪器的基本情况见侯可军等<sup>[42-43]</sup>。激光剥蚀束斑直径为25  $\mu\text{m}$ ,频率为10 Hz,能量密度约为2.5 J/cm<sup>2</sup>,以高纯He为载气。采样方式为单点剥蚀,数据采集采用所有信号同时静态方式接收。锆石年龄采用锆石GJ-1为外标,U、Th含量以锆石M127(U:923×10<sup>-6</sup>, Th:439×10<sup>-6</sup>, Th/U:0.475<sup>[44]</sup>)为外标进行校正,详细的仪器参数设置及分析技术见侯可军等<sup>[45]</sup>。同位素比值和元素含量采用ICPMsDataCal程序<sup>[46]</sup>处理,锆石U-Pb年龄谐和图绘制和加权平均年龄计算(95%置信度)采用Isoplot ver3.23软件<sup>[47]</sup>完成。

Sr、Nd同位素组成测试在中国地质科学院地质研究所同位素实验室完成。Nd同位素测试所用仪器为Nu Plasma HR MC- ICP- MS (Nu Instruments)。测定时,标准溶液和样品溶液在0.1M HCl

介质中由DSN-100型膜去溶进样系统进入,进样速度为50~100  $\mu\text{l}/\text{min}$ 。Nd同位素质量分馏采用 $^{146}\text{Nd}/^{144}\text{Nd}=0.7219$ 校正。标准测定结果:JMC Nd<sub>2</sub>O<sub>3</sub> $^{143}\text{Nd}/^{144}\text{Nd}=0.511124\pm10(2\sigma)$ ,室内标样 $^{143}\text{Nd}/^{144}\text{Nd}=0.512439\pm10(2\sigma)$ 。Sr同位素测试所用仪器为MAT262固体同位素质谱计,质量分馏采用 $^{88}\text{Sr}/^{86}\text{Sr}=8.37521$ 校正,标准测定结果:SRM 987 SrCO<sub>3</sub> $^{87}\text{Sr}/^{86}\text{Sr}=0.710238\pm12(2\sigma)$ 。

#### 3.2 主量、微量元素和稀土元素地球化学

雾岭闪长岩体主量、微量元素和稀土元素分析结果见表1。岩石中性, $\text{SiO}_2$ 含量为56.02%~57.81%(平均56.83%),贫钾, $\text{K}_2\text{O}$ 含量为0.36%~0.5%(平均0.40%)。AR=1.55~1.63, $\delta=1.89\sim1.98$ ,结合AFM图解、Ti-Zr图解和Ti-Zr-Y图解(文中未附)等判断,闪长岩属于钙碱性岩石系列。A/CNK=0.73~0.79,准铝质。在R1-R2图解(图4-a)中投影于板块碰撞前的俯冲消减环境。在MgO-TFeO和CaO-(TFeO+MgO)图解(图4-b,c)中投影于火山弧环境和碰撞环境,不具备板内花岗岩特征。在Y-Nb和(Yb+Nb)-Rb图解(图4-d,e)中落在岛弧区域。在Th-Hf-Ta图解(图4-f)中则落入岛弧钙碱性岩石内。

稀土元素LREE/HREE=3.0~4.3,分馏较弱,轻稀土较为富集,球粒陨石配分曲线平缓右倾(图5-a),无Ce异常,轻度Eu负异常, $\delta\text{Eu}=0.79\sim0.89$ (平均0.84)。相对而言,微量元素明显富集U和Th,亏损K、Nb、Ta和Ti、Zr、Hf、Y、Yb和Lu含量稍低。

#### 3.3 锆石LA-ICP-MS U-Pb年代学

雾岭闪长岩锆石阴极发光图像见图6,测试结果见表2。锆石半自形到自形,粒状到短柱状,粒径一般>100  $\mu\text{m}$ ,震荡环带发育(图6),Th=27~1106  $\mu\text{g/g}$ ,U=49~635  $\mu\text{g/g}$ ,Th/U=0.58~1.77(表2),具有岩浆锆石的特点。19个分析点中有17个 $^{206}\text{Pb}/^{238}\text{U}$ 表面年龄在306~310 Ma,另2个 $^{206}\text{Pb}/^{238}\text{U}$ 表面年龄分别为316.4 Ma和316.6 Ma,年龄十分集中,19个点的 $^{206}\text{Pb}/^{238}\text{U}$ 表面年龄加权平均值为( $307.7\pm0.8$ ) Ma(MSWD=0.77),该值代表了闪长岩的结晶年龄。

#### 3.4 Sr、Nd同位素

雾岭5个闪长岩样品的Sr、Nd同位素组成及特征值见表3。样品的初始Sr同位素较低,为 $^{87}\text{Sr}/^{86}\text{Sr}(t)=$

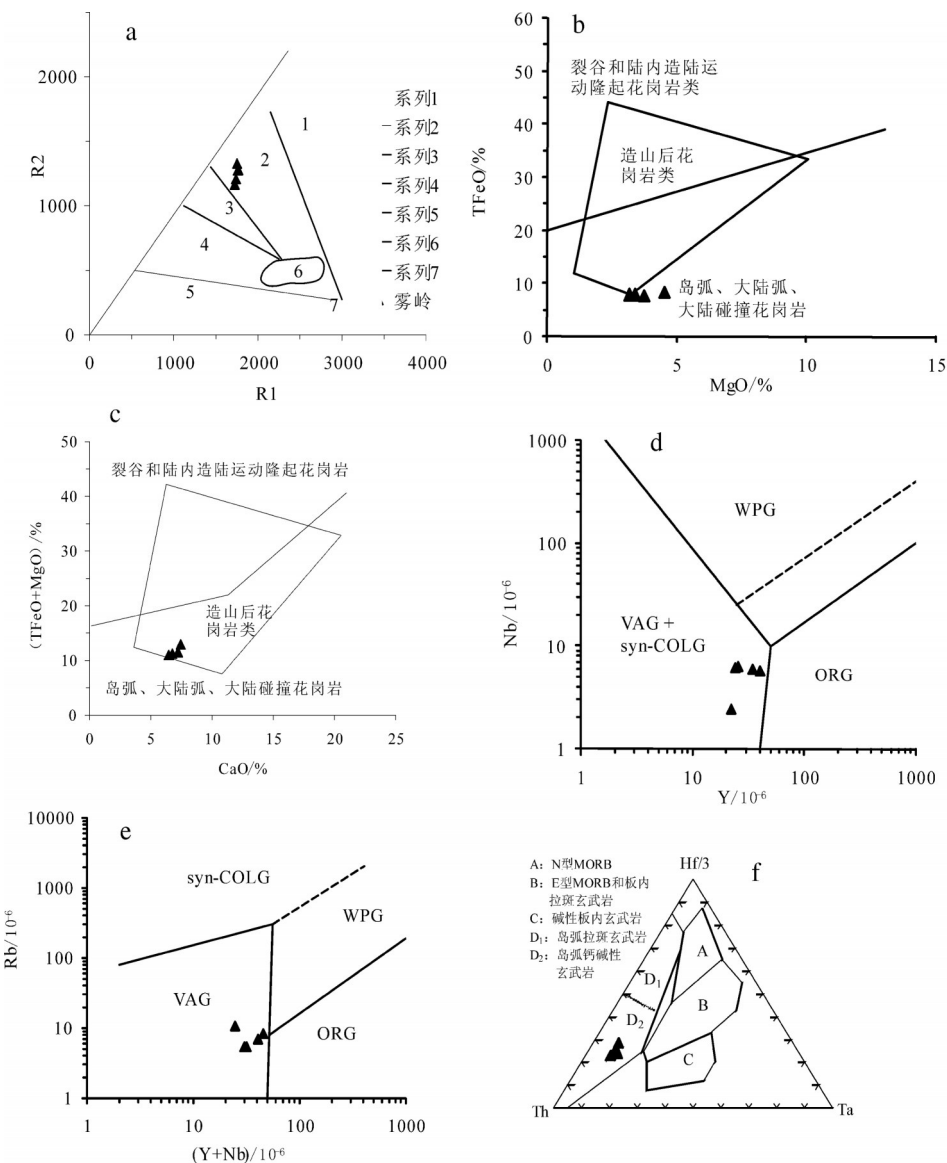


图4 雾岭闪长岩R1-R2(a; 参考文献[48]), TFeO-MgO(b), (TFeO+MgO)-CaO(c; 参考文献[49]), Nb-Y(d), Rb-(Yb+Nb)(e; 参考文献[50])和Th-Hf-Ta(f)图解(参考文献[51])

Fig.4 R1-R2 (a; reference [48]), TFeO-MgO (b), TFeO+MgO-CaO (c; reference [49]), Nb-Y(d), Rb-(Yb+Nb)(e; reference [50]) and Th-Hf-Ta (f) (reference [51]) geotectonic discrimination diagram for the Wuling diorite

0.704279~0.704560;  $\varepsilon_{\text{Nd}}(t)$ 为正值(+3.1~+4.6),明显偏向幔源岩浆特点。计算Nd模式年龄的前提假设是岩石从地幔分离进入大陆地壳后在很短的时间里具有类似大陆地壳的Sm/Nd比值,之后在后期壳内的地质作用中岩石的Sm/Nd比值未改变。样品的 $f(\text{Sm}/\text{Nd})_s$ 较高(为-0.27~-0.15),明显不同于一般地壳岩石的 $f(\text{Sm}/\text{Nd})$ (-0.3~-0.5),显示岩浆源区更富Sm贫Nd,单阶段Nd模式年龄会明显偏老,因

此使用二阶段演化方程计算Nd模式年龄,得到 $T_{\text{2DM}}=695 \sim 818 \text{ Ma}$ 。

## 4 讨 论

### 4.1 岩浆源区特征

雾岭闪长岩具有正的 $\varepsilon_{\text{Nd}}(t)$ 值(3.1~4.6)和相对低的初始 $^{87}\text{Sr}/^{86}\text{Sr}$ 比值(0.7043~0.7046),Nd模式年龄为695~818 Ma,在 $^{87}\text{Sr}/^{86}\text{Sr}(t)-\varepsilon_{\text{Nd}}(t)$ 图解上位于地

表1 闪长岩主量元素(%)、微量元素( $10^6$ )组成Table 1 Major element (%) and trace element ( $10^6$ ) compositions of the Wuling diorite

项目	WL-19	WL-20	WL-21	WL-26	WL-27	项目	WL-19	WL-20	WL-21	WL-26	WL-27
SiO <sub>2</sub>	56.02	57.81	56.54	56.39	57.39	Sr	303	312	350	336	329
Al <sub>2</sub> O <sub>3</sub>	15.71	16.16	16.35	16.34	16.26	Zr	74.7	83.1	116	130	121
TiO <sub>2</sub>	0.93	1.1	1.15	1.14	1.12	Hf	2.19	2.59	3.29	3.61	3.3
CaO	7.44	6.47	7.23	7.21	6.76	Th	1.61	2.32	2.97	3.18	3.24
Fe <sub>2</sub> O <sub>3</sub>	4.1	4.34	3.81	3.63	4.59	U	0.5	1.61	0.73	0.78	1.28
FeO	4.74	3.95	4.38	4.54	3.74	Nb	2.47	5.81	6.4	6.23	6.03
K <sub>2</sub> O	0.5	0.36	0.38	0.38	0.37	Ta	0.23	0.38	0.46	0.45	0.41
Na <sub>2</sub> O	4.51	5.05	4.68	4.67	4.92	Y	22	39.7	25.3	23.9	34.1
MgO	4.51	3.14	3.72	3.72	3.37	La	9.52	12.5	13.2	12.6	12.5
MnO	0.14	0.12	0.13	0.13	0.12	Ce	20.4	32	31.1	29.8	31
P <sub>2</sub> O <sub>5</sub>	0.16	0.24	0.35	0.35	0.28	Pr	2.6	4.57	4.09	4.01	4.28
CO <sub>2</sub>	0.6	0.26	0.34	0.17	0.26	Nd	11.4	20.4	17.2	17	19.1
H <sub>2</sub> O+	1	0.72	0.84	0.96	0.84	Sm	3.02	5.62	4.05	4.15	4.89
LOI	1.23	0.83	0.93	0.84	0.76	Eu	0.96	1.57	1.18	1.14	1.43
Total	101.59	100.55	100.83	100.47	100.78	Gd	3.59	6.5	4.3	4.53	5.52
A/CNK	0.73	0.79	0.77	0.77	0.78	Tb	0.6	1.06	0.71	0.7	0.94
AR	1.55	1.63	1.55	1.55	1.60	Dy	3.78	6.85	4.37	4.34	5.83
$\delta$	1.93	1.98	1.89	1.90	1.94	Ho	0.82	1.47	0.92	0.9	1.24
K <sub>2</sub> O/Na <sub>2</sub> O	0.11	0.07	0.08	0.08	0.08	Er	2.53	4.46	2.79	2.72	3.8
Ti	5631	7118	7134	7093	7110	Tm	0.33	0.62	0.38	0.37	0.52
V	307	278	317	313	293	Yb	2.23	4.13	2.6	2.48	3.36
Cr	14.6	25.2	17.6	17.6	24.5	Lu	0.34	0.59	0.4	0.39	0.54
Zn	48.9	40.9	38	37.1	39.2	$\Sigma$ REE	62.12	102.34	87.29	85.13	94.95
Ga	15.5	17.1	16.1	15.7	17.3	LREE/HREE	3.37	2.99	4.30	4.18	3.37
Ba	119	105	140	136	122	La <sub>N</sub> /Yb <sub>N</sub>	2.88	2.04	3.42	3.43	2.51
Rb	10.4	8.2	5.33	5.3	6.78	$\delta$ Eu	0.89	0.79	0.86	0.80	0.84
						$\delta$ Ce	0.97	1.02	1.01	1.00	1.02

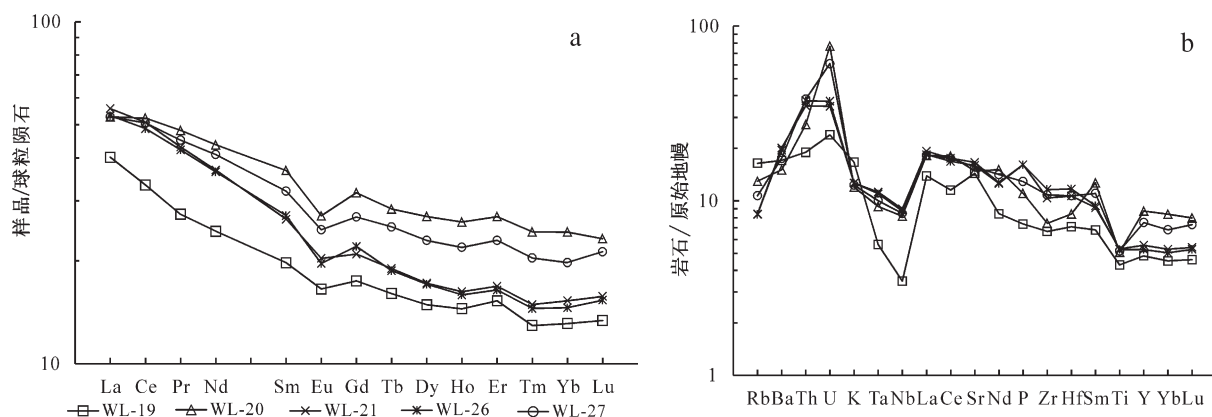


图5 雾岭岩体闪长岩稀土元素球粒陨石标准化配分图(a)和原始地幔标准化的微量元素蛛网图(b; 标准自参考文献[52])  
Fig.5 Chondrite-normalized REE patterns (a) and primitive mantle-normalized trace element spider diagram (b; reference [52]) of the Wuling magnetite mineralized diorite

幔趋势线上(图8),表明地幔是闪长岩的源区。地幔来源闪长岩一般认为有以下3种成因:①由玄武质岩浆与地壳物质相互作用而发生分离结晶作用形成<sup>[55]</sup>;②由更深部地幔橄榄岩在含水条件下部分熔融形成;③由玄武质岩浆与酸性岩浆混合作用形

成。地幔(包括原始地幔、亏损地幔和富集地幔)的Th、Ta丰度很低, Th/Ta比值大致相等。地幔中Th的丰度仅为0.05  $\mu\text{g/g}$ <sup>[56]</sup>, 岛弧玄武岩的Th平均约0.27  $\mu\text{g/g}$ <sup>[57]</sup>, 而陆壳(尤其是花岗岩)中的Th含量最高, 达16~21  $\mu\text{g/g}$ <sup>[58]</sup>。雾岭闪长岩的Th含量较高,

表2 雾岭铁矿闪长岩锆石LA-ICP-MS U-Pb测年分析结果

Table 2 LA-ICP-MS U-Pb analytical results of zircon from diorite of the Wuling iron deposit

测点号	含量/ $10^{-6}$		同位素比值						表面年龄/Ma					
	Pb	$^{232}\text{Th}$	$^{238}\text{U}$	Th/U	$^{207}\text{Pb}/^{206}\text{Pb}$	$1\sigma$	$^{207}\text{Pb}/^{235}\text{U}$	$1\sigma$	$^{208}\text{Pb}/^{232}\text{Th}$	$1\sigma$	$^{207}\text{Pb}/^{206}\text{Pb}$	$1\sigma$	$^{206}\text{Pb}/^{238}\text{U}$	$1\sigma$
WL-21-1	84	46	56	0.83	0.05556	0.00192	0.3848	0.0132	0.05033	0.00037	0.00545	0.00081	435.2	71.3
WL-21-2	698	439	371	1.18	0.05275	0.00029	0.3581	0.0024	0.04924	0.00019	0.00168	0.00014	316.7	13.0
WL-21-3	98	71	88	0.81	0.05304	0.00080	0.3565	0.0053	0.04882	0.00020	0.00257	0.00031	331.5	35.2
WL-21-4	1068	478	271	1.77	0.05309	0.00035	0.3565	0.0027	0.04871	0.00019	0.00121	0.00018	331.5	14.8
WL-21-5	348	137	176	0.78	0.05252	0.00046	0.3523	0.0034	0.04864	0.00018	0.00140	0.00027	309.3	20.4
WL-21-6	933	372	243	1.53	0.05249	0.00037	0.3519	0.0032	0.04865	0.00031	0.00089	0.00021	305.6	12.0
WL-21-7	582	232	172	1.35	0.05272	0.00055	0.3541	0.0044	0.04874	0.00035	0.00090	0.00028	316.7	19.4
WL-21-8	672	240	167	1.43	0.05528	0.00138	0.3743	0.0111	0.04894	0.00039	0.00068	0.00028	433.4	55.6
WL-21-9	1104	340	257	1.32	0.05260	0.00037	0.3538	0.0039	0.04883	0.00045	0.00055	0.00030	322.3	16.7
WL-21-10	212	63	75	0.84	0.05304	0.00090	0.3565	0.0066	0.04872	0.00035	0.00139	0.00061	331.5	34.3
WL-21-11	236	77	121	0.63	0.05256	0.00059	0.3534	0.0045	0.04875	0.00029	0.00139	0.00048	309.3	30.6
WL-21-12	262	93	136	0.69	0.05261	0.00054	0.3553	0.0042	0.04903	0.00032	0.00173	0.00047	322.3	28.7
WL-21-13	659	149	182	0.82	0.05261	0.00047	0.3541	0.0040	0.04880	0.00030	0.00160	0.00035	322.3	15.7
WL-21-14	430	126	117	1.07	0.05298	0.00059	0.3593	0.0040	0.04926	0.00024	0.00174	0.00032	327.8	25.9
WL-21-15	96	27	49	0.55	0.05272	0.00128	0.3557	0.0083	0.04908	0.00026	0.00594	0.00096	316.7	55.6
WL-21-16	14	33	50	0.67	0.05007	0.00103	0.3362	0.0074	0.04863	0.00033	0.00434	0.00067	198.2	52.8
WL-21-17	3651	1106	635	1.74	0.05268	0.00022	0.3655	0.0031	0.05031	0.00038	0.00171	0.00019	322.3	9.3
WL-21-18	457	133	136	0.98	0.05284	0.00052	0.3588	0.0043	0.04928	0.00039	0.00247	0.00030	320.4	22.2
WL-21-19	444	155	165	0.94	0.05403	0.00048	0.3648	0.0040	0.04899	0.00037	0.00221	0.00027	372.3	18.5

表3 雾岭铁矿闪长岩Sr、Nd同位素组成( $10^{-6}$ )和特征参数  
Table 3 Sr and Nd isotopic compositions ( $10^{-6}$ ) and characteristic parameters of the Wuling diorite

#号	Rb/ $10^{-6}$	Sr/ $10^{-6}$	$^{87}\text{Rb}/^{86}\text{Sr}$	$^{87}\text{Sr}/^{86}\text{Sr}$	$2\sigma$	$^{87}\text{Sr}/^{86}\text{Sr}_{\text{t}}$	$\text{Sm}/10^{-6}$	$\text{Nd}/10^{-6}$	$^{147}\text{Sm}/^{144}\text{Nd}$	$2\sigma$	$^{143}\text{Nd}/^{144}\text{Nd}_{\text{t}}$	$\varepsilon_{\text{Nd}}(\text{t})$	$f(\text{Sm}/\text{Nd})_{\text{s}}$	$T_{\text{DM}}/\text{Ma}$	$T_{\text{DDM}}/\text{Ma}$	
WL-19	10.4	303	0.10	0.704773	14	0.704337	3.02	11.4	0.16	0.512801	5	0.5124761	4.6	-0.18	1014	695
WL-20	8.2	312	0.08	0.704613	13	0.704279	5.62	20.4	0.17	0.512793	5	0.5124551	4.2	-0.15	1181	728
WL-21	5.33	350	0.04	0.704740	15	0.704547	4.05	17.2	0.14	0.512695	6	0.5124062	3.2	-0.27	986	806
WL-26	5.3	336	0.05	0.704760	14	0.704560	4.15	17	0.15	0.512698	12	0.5123986	3.1	-0.25	1058	818
WL-27	6.78	329	0.06	0.704676	14	0.704414	4.89	19.1	0.16	0.512756	5	0.512442	3.9	-0.21	1037	749

Note: Chondrite uniform reservoir (CHUR) values [ $(^{143}\text{Sm}/^{144}\text{Nd})_{\text{CHUR}0} = 0.512638$ ,  $(^{143}\text{Nd}/^{144}\text{Nd})_{\text{CHUR}0} = 0.1967$ ] and depleted mantle (DM) values [ $(^{143}\text{Sm}/^{144}\text{Nd})_{\text{DM}} = 0.513151$ ,  $(^{143}\text{Nd}/^{144}\text{Nd})_{\text{DM}} = 0.2137$ ] are used for the calculation.  $f_{\text{Sm}, \text{Nd}} = (^{147}\text{Sm}/^{144}\text{Nd})_{\text{DM}} / (^{147}\text{Sm}/^{144}\text{Nd})_{\text{CHUR}0} - 1$ .  $\lambda_{\text{Rb}} = 1.42 \times 10^{-11}/\text{year}$  (Reference [53]) and  $\lambda_{\text{Sm}} = 6.54 \times 10^{-12}/\text{year}$  (Reference [54]). The initial Sr and Nd isotopic ratios were corrected to 304 Ma, 304 Ma, 312 Ma, 300 Ma and 299 Ma for rhyolite, dacite granite, diabase dyke, and diorite dyke, respectively.

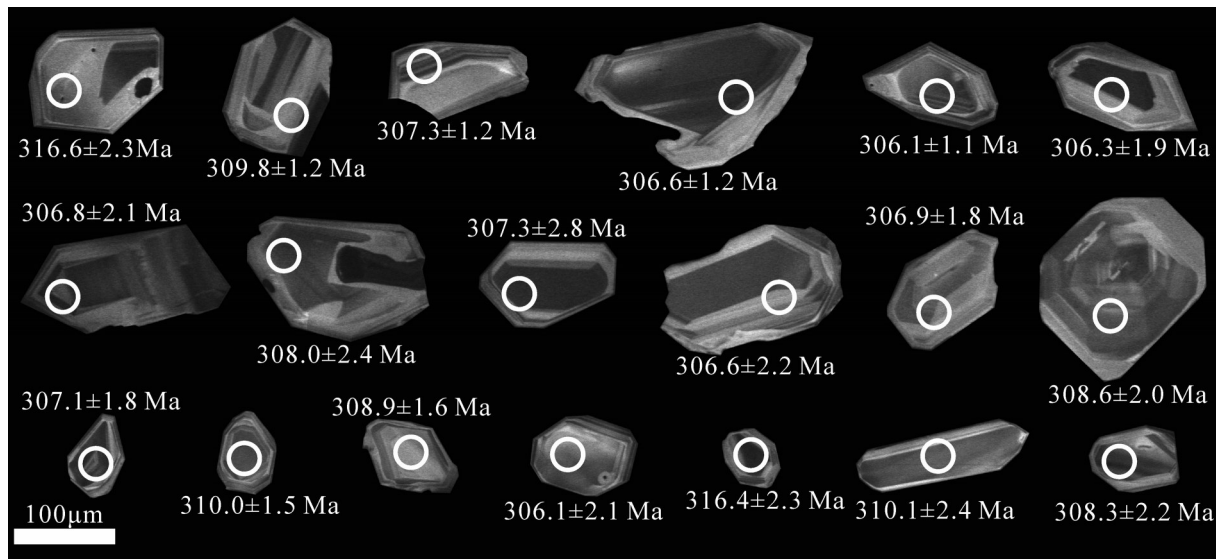


图6 雾岭铁矿闪长岩部分锆石阴极发光(CL)图像及测试位置  
Fig.6 Cathodoluminescence (CL) images of selected zircons from the Wuling diorite sample

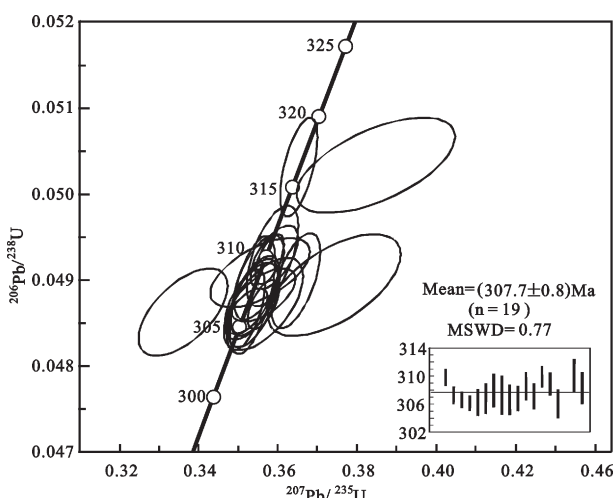


图7 雾岭闪长岩锆石U-Pb谐和图  
Fig.7 U-Pb concordia diagram of zircons from the Wuling diorite

在 $1.61 \sim 3.24 \mu\text{g/g}$ , Th/Ta比值也高,为 $6.1 \sim 7.9$ ,显然受到了陆壳混染作用的影响。雾岭闪长岩的初始 $^{87}\text{Sr}/^{86}\text{Sr}$ 和 $\varepsilon_{\text{Nd}}(t)$ 组成介于地幔和西天山下地壳之间,也支持地幔来源岩浆受地壳混染作用的认识。因此,假说②不适合解释雾岭闪长质岩浆的成因。雾岭闪长岩体内未观察到岩浆混合证据,闪长岩的化学成分也比较稳定,假说③也不适合解释雾岭闪长质岩浆的成因。由此认为,雾岭闪长岩岩浆可能

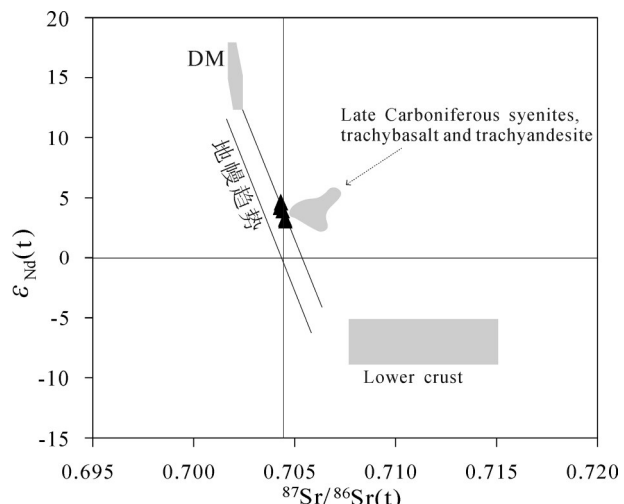


图8 雾岭岩体闪长岩 $^{87}\text{Sr}/^{86}\text{Sr}(t)-\varepsilon_{\text{Nd}}(t)$ 图  
数据来源:晚石炭世正长岩、粗面玄武岩和玄武岩自文献[13],DM自文献[59],下地壳自文献[60,61]  
Fig. 8 Diagram of  $^{87}\text{Sr}/^{86}\text{Sr}(t)$  versus  $\varepsilon_{\text{Nd}}(t)$  for the Wuling diorite  
Data sources: late Carboniferous syenites, trachybasalts and trachyandesites (reference [13]); DM (reference [59]); lower crust (reference [60,61])

是由玄武质岩浆与地壳物质相互作用而发生分离结晶作用所形成。

#### 4.2 雾岭闪长岩的构造环境

雾岭闪长岩所在的阿吾拉勒铁矿带位于西天山伊犁微陆块之上。该陆块约在距今700 Ma左右由

Rodinia超大陆裂解而来<sup>[16]</sup>。伊犁微陆块在石炭纪早期南北曾分别受南天山洋和北天山洋洋壳的俯冲,为一种具有陆壳基底的火山弧环境<sup>[12, 17–18]</sup>。其两侧的蛇绿岩年龄被限定在早石炭世及以前<sup>[62–67]</sup>。位于伊犁微陆块南侧的“西天山高压增生楔”峰期变质发生在早石炭世末,结合花岗岩类等的大量研究表明,西天山在早石炭世末结束增生造山作用<sup>[12]</sup>。伊犁微陆块二叠纪火山岩和侵入岩岩石组合和地球化学特点显示形成于伸展的构造背景<sup>[68–74]</sup>。在晚石炭世伊犁微陆块由于与塔里木板块发生块体间旋转<sup>[19,21]</sup>,剪切应力可能使伊犁微陆块内发生了造山带根部拆沉<sup>[13,40]</sup>和局部形成的挤压–伸展的构造转变<sup>[9]</sup>等,并造就了阿吾拉勒海相火山岩型铁矿带。雾岭闪长岩锆石U–Pb年龄为(307.7±0.8)Ma,是晚石炭世侵入的,正是在这种背景下形成。

雾岭闪长岩在增生造山作用结束之后侵入,属板内岩浆作用,但保留了岛弧火山岩的印记,如在多种构造环境判别图解中投影于岛弧区域(图4),相对富集U和Th等大离子亲石元素,相对亏损Nb、Ta、Zr、Hf等高场强元素。相似的闪长岩在北祁连造山带也有发现<sup>[75]</sup>,并认为可能是受亏损地幔源区和陆壳混染作用的双重影响所致。一方面,增生造山刚结束,伊犁微陆块深部的地幔源区可能仍保存有消减带之上的地幔楔的特点;另一方面,源于该地幔源区的岩浆上升时与陆壳发生混染。

## 5 结 论

雾岭闪长岩锆石U–Pb年龄为(307.7±0.8)Ma,是在西天山增生造山结束、伊犁微陆块与塔里木板块发生块体间旋转时侵位的,属于增生造山后的产物,其成因可能与伊犁微陆块内造山带根部拆沉作用或局部形成的挤压–伸展的构造转变带有关。雾岭闪长岩在板内环境产生,保留有岛弧岩浆作用的痕迹,与北祁连老虎山闪长岩相似,可能是受岩浆源区和陆壳混染双重影响的结果。

致谢:在野外工作中得到了新疆地矿局第三地质大队张永平工程师的帮助,在此致以衷心的感谢!感谢审稿人对本文的评论和提出的修改意见。

## 参考文献(References):

- [1] Sengör A. Evolution of the Altai tectonic collage and Palaeozoic crustal growth in Eurasia [J]. Nature, 1993, 364: 299–307.
- [2] Jahn B M, Wu F Y, Chen B. Massive granitoid generation in Central Asia: Nd isotope evidence and implication for continental growth in the Phanerozoic [J]. Episodes, 2000, 23: 82–92.
- [3] Xiao W J, Han C M, Yuan C, et al. Middle Cambrian to Permian subduction–related accretionary orogenesis of Northern Xinjiang, NW China: Implications for the tectonic evolution of central Asia [J]. Journal of Asian Earth Sciences, 2008, 32: 102–117.
- [4] Xiao W J, Shu L S, Gao J, et al. Geodynamic processes of the Central Asian Orogenic Belt and its metallogeny [J]. China Basic Science, 2009, (3): 13–19.
- [5] Zhang X, Tian J Q, Gao J, et al. Geochronology and geochemistry of granitoid rocks from the Zhibo syngenetic volcanogenic iron ore deposit in the Western Tianshan Mountains (NW–China): Constraints on the age of mineralization and tectonic setting[J]. Gondwana Research, 2012, 22(2): 585–596.
- [6] 王登红, 李纯杰, 陈郑辉, 等. 东天山成矿规律与找矿方向的初步研究[J]. 地质通报, 2006, 25(8): 910–915.  
Wang DENGHONG, Li Chunjie, Chen Zhenghui, et al. Metallogenetic characteristics and direction in mineral search in the East Tianshan, Xinjiang, China[J]. Geological Bulletin of China, 2006, 25(8): 910–915 (in Chinese with English abstract).
- [7] 陈毓川, 刘德权, 唐延龄, 等. 中国天山矿产及成矿体系(上册)[M]. 北京: 地质出版社, 2008: 243–287.  
Chen YUCHUAN, Liu Dequan, Tang Yanling, et al. Mineral Resources and Mineralization System in Tianshan, China (Vol. 1) [M]. Beijing: Geological Publishing House, 2008: 246–287 (in Chinese with English abstract).
- [8] 杨富全, 刘锋, 柴凤梅, 等. 新疆阿尔泰铁矿地质特征、时空分布及成矿作用[J]. 矿床地质, 2011, 30(4): 575–598.  
Yang Fuquan, Liu Feng, Chai Fengmei, et al. Iron deposits in Altay, Xinjiang: Geological characteristics, time–space distribution and metallogenesis[J]. Mineral Deposits, 2011, 30(4): 575–598 (in Chinese with English abstract).
- [9] 张作衡, 洪为, 蒋宗胜, 等. 新疆西天山晚古生代铁矿床的地质特征、矿化类型及形成环境[J]. 矿床地质, 2012, 31(5): 941–964.  
Zhang Zuoheng, Hong Wei, Jiang Zongsheng, et al. Geological features, mineralization types and metallogenic setting of Late Paleozoic iron deposits in western Tianshan Mountains of Xinjiang[J]. Mineral Deposits, 2012, 31(5): 941–964 (in Chinese with English abstract).
- [10] 洪为, 张作衡, 李华芹, 等. 新疆西天山查岗尔铁矿床成矿时代——来自石榴子石Sm–Nd等时线年龄的信息[J]. 矿床地质, 2012, 31(5): 1067–1074.  
Hong Wei, Zhang Zuoheng, Li Huaqin, et al. Metallogenic epoch of Chagangnuoer iron deposit in western Tianshan Mountains, Xinjiang: Information for garnet Sm–Nd isochron age[J]. Mineral Deposits, 2012, 31(5): 1067–1074 (in Chinese with English abstract).
- [11] 段圣国, 张志海, 江志生, 等. 地质学, 地球化学, 2014, 41(6)

- and geochronology of the Dunde iron-zinc ore deposit in western Tianshan, China[J]. *Ore Geology Reviews*, 2014, 57:441–461.
- [12] 高俊, 钱青, 龙灵利, 等. 西天山的增生造山过程[J]. 地质通报, 2009, 28(12): 1804–1816.  
Gao Jun, Qian Qing, Long Lingli, et al. Accretionary orogenic process of Western Tianshan, China[J]. *Geological Bulletin of China*, 2009, 28(12): 1804–1816 (in Chinese with English abstract).
- [13] Sun L H, Wang Y J, Fan W M, et al. Post-collisional potassic magmatism in the Southern Awulale Mountain, western Tianshan Orogen: Petrogenetic and tectonic implications[J]. *Gondwana Research*, 2008, 14: 383–394.
- [14] Tang G J, Wang Q, Wyman D A, et al. Geochronology and geochemistry of Late Paleozoic magmatic rocks in the Lamasu-Dabate area, northwestern Tianshan (west China): evidence for a tectonic transition from arc to post-collisional setting[J]. *Lithos*, 2010, 119: 393–411.
- [15] Kröner A, Windley B F, Badarch G, et al. Accretionary growth and crust formation in the Central Asian Orogenic Belt and comparison with the Arabian-Nubian shield[J]. *Geological Society of America Memoirs*, 2007, 200: 181–209.
- [16] 左国朝, 张作衡, 王志良, 等. 新疆西天山地区构造单元划分、地层系统及其构造演化[J]. 地质论评, 2008, 54(6):748–767.  
Zuo Guochao, Zhang Zuoheng, Wang Zhiliang, et al. Tectonic division, stratigraphical system and evolution of Western Tianshan Mountains, Xinjiang[J]. *Geological Review*, 2008, 54(6): 748–767 (in Chinese with English abstract).
- [17] Gao J, Long L L, Klemd R, et al. Tectonic evolution of the South Tianshan orogen and adjacent regions, NW China: geochemical and age constraints of granitoid rocks[J]. *International Journal of Earth Sciences*, 2009, 98: 1221–1238.
- [18] Long L L, Gao J, Klemd R, et al. Geochemical and geochronological studies of granitoid rocks from the Western Tianshan Orogen: Implications for continental growth in the southwestern Central Asian Orogenic Belt[J]. *Lithos*, 2011, 126: 321–340.
- [19] Chen C M, Lu H F, Jia D, et al. Closing history of the southern Tianshan oceanic basin, Western China: an oblique collisional orogeny[J]. *Tectonophysics*, 1999, 302: 23–40.
- [20] 段士刚. 新疆西天山赛里木微地块区域成矿规律与找矿方向[D]. 中国地质大学(北京), 2011: 1–192.  
Duan Shigang. Regional Metallogenic Regularity and Prospecting Direction of Sailimu Micro-massif, Western Tianshan, China[J]. Beijing: China University of Geoscience, 2011: 1–192 (in Chinese with English abstract).
- [21] Wang B, Chen Y, Zhan S, et al. Primary Carboniferous and Permian paleomagnetic results from the Yili Block (NW China) and their implications on the geodynamic evolution of Chinese Tianshan Belt[J]. *Earth and Planetary Science Letters*, 2007, 263: 288–308.
- [22] Bazhenov M L, Collins A Q, Degtyarev K E, et al. Paleozoic northward drift of the North Tien Shan (Central Asia) as revealed by Ordovician and Carboniferous paleomagnetism[J]. *Tectonophysics*, 2003, 366: 113–141.
- [23] Allen M B, Windley B F, Zhang C. Palaeozoic collisional tectonics and magmatism of the Chinese Tien Shan, central Asia[J]. *Tectonophysics*, 1992, 220: 89–115.
- [24] Windley B F, Allen M B, Zhang C, et al. Paleoizoic accretion and Cenozoic reformation of the Chinese Tien Shan range, central Asia[J]. *Geology*, 1990, 18: 128–131.
- [25] 王强, 赵振华, 许继峰, 等. 天山北部石炭纪埃达克岩-高镁安山岩-富Nb岛弧玄武质岩: 对中亚造山带显生宙地壳增生与铜金成矿的意义[J]. 岩石学报, 2006, 22(1):11–30.  
Wang Qiang, Zhao Zhenhua, Xu Jifeng, et al. Carboniferous adakite-high-Mg andesite-Nb-enriched basaltic rock suites in the Northern Tianshan area: Implications for phanerozoic crustal growth in the Central Asia Orogenic Belt and Cu-Au mineralization[J]. *Acta Petrologica Sinica*, 2006, 22(1): 11–30 (in Chinese with English abstract).
- [26] Wang B, Shu L S, Cluzel D, et al. Geochemical constraints on Carboniferous volcanic rocks of the Yili Block (Xinjiang, NW China): Implication for the tectonic evolution of Western Tianshan[J]. *Journal of Asian Earth Sciences*, 2007, 29:148–159.
- [27] 袁新东, 张兵, 高永利, 等. 西天山阿吾拉勒地区石炭系划分对比新资料[J]. 新疆地质, 2008, 26(3): 231–235.  
Luan Xindong, Zhang Bing, Gao Yongli, et al. New materials of stratigraphic classification and correlation of the Carboniferous in Awulale area, Western Tianshan[J]. *Xinjiang Geology*, 2008, 26(3): 231–235 (in Chinese with English abstract).
- [28] 李永军, 李注苍, 周继兵, 等. 西天山阿吾拉勒一带石炭系岩石地层单位厘定[J]. 岩石学报, 2009, 25(6): 1332–1340.  
Li Yongjun, Li Zhucang, Zhou Jibing, et al. Division of the Carboniferous lithostratigraphic units in Awulale area, western Tianshan[J]. *Acta Petrologica Sinica*, 2009, 25(6):1332–1340 (in Chinese with English abstract).
- [29] 李永军, 高永利, 佟丽莉, 等. 西天山阿吾拉勒一带石炭系阿克沙克组风暴岩及其意义[J]. 地学前缘, 2009, 16(3): 341–348.  
Li Yongjun, Gao Yongli, Tong Lili, et al. Tempestite of Akeshake Formation in Awulale area, Western Tianshan and its significance[J]. *Earth Science Frontiers*, 2009, 16(3): 341–348 (in Chinese with English abstract).
- [30] 冯金星, 石福品, 汪帮耀, 等. 西天山阿吾拉勒成矿带火山岩型铁矿[M]. 北京: 地质出版社, 2010: 10–150.  
Feng Jinxing, Shi Fupin, Wang Bangyao, et al. Volcanogenic iron Deposits in the Awulale Metallogenic Belt in Western Tianshan[M]. Beijing: Geological Publishing House, 2010: 10–150 (in Chinese).
- [31] 朱永峰, 张立飞, 古丽冰, 等. 西天山石炭纪火山岩 SHRIMP 年

- 代学及其微量元素地球化学研究[J]. 科学通报, 2005, 50(18): 2004–2014.
- Zhu Yongfeng, Zhang Lifei, Gu Libing, et al. SHRIMP dating and trace element geochemistry of Carboniferous volcanic rocks in Western Tianshan[J]. Chinese Science Bulletin, 2005, 50(18): 2004–2014(in Chinese).
- [32] 朱永峰, 周晶, 宋彪, 等. 新疆“大哈拉军山组”火山岩的形成时代问题及其解体方案[J]. 中国地质, 2006, 33(3): 487–497.
- Zhu Yongfeng, Zhou Jing, Song Biao, et al. Age of the “Dahalajunshan” Formation in Xinjiang and its disintegration[J]. Geology in China, 2006, 33(3): 487–497 (in Chinese with English abstract).
- [33] 朱永峰, 周晶, 郭璇. 西天山石炭纪火山岩岩石学及Sr–Nd同位素地球化学研究[J]. 岩石学报, 2006, 22(5): 1341–1350.
- Zhu Yongfeng, Zhou Jing, Guo Xuan. Petrology and Sr–Nd isotopic geochemistry of the Carboniferous volcanic rocks in the western Tianshan Mountains, NW China[J]. Acta Petrologica Sinica, 2006, 22(5): 1341–1350 (in Chinese with English abstract).
- [34] 翟伟, 孙晓明, 高俊, 等. 新疆阿希金矿床赋矿围岩——大哈拉军山组火山岩 SHRIMP 锆石年龄及其地质意义[J]. 岩石学报, 2006, 22(5): 1399–1404.
- Zhai Wei, Sun Xiaoming, Gao Jun, et al. SHRIMP dating of zircons from volcanic host rocks of Dahalajunshan Formation in Axi gold deposit, Xinjiang, China, and its geological implications[J]. Acta Petrologica Sinica, 2006, 22(5): 1399–1404 (in Chinese with English abstract).
- [35] 安芳, 朱永峰. 西北天山吐拉苏盆地火山岩 SHRIMP 年代学和微量元素地球化学研究[J]. 岩石学报, 2008, 24(12): 2741–2748.
- An Fang, Zhu Yongfeng. Study on trace elements geochemistry and SHRIMP chronology of volcanic rocks in Tulasu Basin, Northwest Tianshan[J]. Acta Petrologica Sinica, 2008, 24(12): 2741–2748 (in Chinese with English abstract).
- [36] 蒋宗胜, 张作衡, 侯可军, 等. 西天山查岗诺尔和智博铁矿区火山岩地球化学特征、锆石 U–Pb 年龄及地质意义[J]. 岩石学报, 2012, 28(7): 2074–2088.
- Jiang Zongsheng, Zhang Zuoheng, Hou Kejun, et al. Geochemistry and zircon U–Pb age of volcanic rocks from the Chagangnuoer and Zhibo iron deposits, western Tianshan, and their geological significance[J]. Acta Petrologica Sinica, 2012, 28(7): 2074–2088 (in Chinese with English abstract).
- [37] 张玄杰, 郑广如, 范子梁, 等. 新疆西天山东段航磁推断断裂构造特征[J]. 物探与化探, 2011, 35(4): 448–454.
- Zhang Xuanjie, Zheng Guangru, Fan Ziliang, et al. Structural characteristics of aeromagnetic deduced faults in Western Tianshan Mountains, Xinjiang[J]. Geophysical and Geochemical Exploration, 2011, 35(4): 448–454 (in Chinese with English abstract).
- [38] 李永军, 杨高学, 郭文杰, 等. 西天山阿吾拉勒阔尔库岩基的解体及地质意义[J]. 新疆地质, 2007, 25(3): 233–236.
- Li Yongjun, Yang Gaoxue, Guo Wenjie, et al. The disintegration and geological significance of the Kuoerku granite batholiths in Awulale, Western Tianshan[J]. Xinjiang Geology, 2007, 25(3): 233–236 (in Chinese with English abstract).
- [39] 杨高学, 周继兵, 栾新东, 等. 西天山阿吾拉勒阔尔库岩基解体的地球化学证据及意义[J]. 新疆地质, 2008, 26(2): 128–132.
- Yang Gaoxue, Zhou Jibing, Luan Xindong, et al. The geochemical evidence and its significance of the “disintegration” of the Kuoerku granite batholith in Awulale, western Tianshan[J]. Xinjiang Geology, 2008, 26(2): 128–132 (in Chinese with English abstract).
- [40] Zhang Z H, Hong W, Jiang Z S, et al. Geological characteristics and zircon U–Pb dating of volcanic rocks from the Beizhan iron deposit in western Tianshan Mountains, Xinjiang, NW China [J]. Acta Geologica Sinica, 2012, 86(3): 737–747.
- [41] Zhao Z H, Xiong X L, Wang Q, et al. Underplating–related adakites in Xinjiang Tianshan, China[J]. Lithos, 2008, 102: 74–391.
- [42] 侯可军, 李延河, 邹天人, 等. LA–MC–ICP–MS 锆石 Hf 同位素的分析方法及地质应用[J]. 岩石学报, 2007, 23(10): 2595–2604.
- Hou Kejun, Li Yanhe, Zou Tianren, et al. Laser ablation–MC–ICP–MS technique for Hf isotope microanalysis of zircon and its geological applications[J]. Acta Petrologica Sinica, 2007, 23(10): 2595–2604 (in Chinese with English abstract).
- [43] 侯可军, 李延河, 田有荣, 等. MC–ICP–MS 高精度 Cu、Zn 同位素测试技术[J]. 矿床地质, 2008, 27(6): 774–781.
- Hou Kejun, Li Yanhe, Tian Yourong, et al. High precision Cu,Zn isotope measurements by multi– collector ICP– MS[J]. Mineral Deposits, 2008, 27(6): 774–781 (in Chinese with English abstract).
- [44] Nasdala L, Hofmeister W, Norberg N, et al. Zircon M257: A homogeneous natural reference material for the ion microprobe U–Pb analysis of zircon[J]. Geostandards and Geoanalytical Research, 2008, 32: 247–265.
- [45] 侯可军, 李延河, 田有荣. LA–MC–ICP–MS 锆石微区原位 U–Pb 定年技术[J]. 矿床地质, 2009, 28(4): 481–492.
- Hou Kejun, Li Yanhe, Tian Yourong. In situ U–Pb zircon dating using laser ablation–multi ion counting–ICP–MS[J]. Mineral Deposits, 2009, 28(4): 481–492 (in Chinese with English abstract).
- [46] Liu Y S, Gao S, Hu Z C, et al. Continental and oceanic crust recycling– induced melt– peridotite interactions in the Trans–North China Orogen: U–Pb dating, Hf isotopes and trace elements in zircons from mantle xenoliths[J]. Journal of Petrology, 2010, 51: 537–571.
- [47] Ludwig K R. User's manual for Isoplot 3.00: A geochronological toolkit for Microsoft Excel. Berkeley Geochronology Center, Special Publication, 2003, (4): 37–41.

- [48] Batchelor R A, Bowden P. Petrogenetic interpretation of granitoid rock series using multicationic parameters[J]. *Chemical Geology*, 1985, 48: 43–55.
- [49] Maniar P D, Piccoli P M. Tectonic discrimination of granitoids[J]. *Geol. Soc. Am. Bull.*, 1989, 101: 635–643.
- [50] Pearce J A, Harris N B W, Tindle A G. Trace element discrimination diagrams for the tectonic interpretation of granitic rocks[J]. *Journal of Petrology*, 1984, 25: 956–983.
- [51] Wood D A. The application of a Th–Hf–Ta diagram to problems of tectonomagmatic classification and to establishing the nature of crustal contamination of basaltic lavas of the British Tertiary Volcanic Province[J]. *Earth and Planetary Science Letters*, 1980, 50: 11–30.
- [52] Sun S S, McDonough W F. Chemical and isotopic systematics of oceanic basalts: implication for mantle composition and process[J]. Geological Society, London, Special Publications, 1989, 42: 313–345.
- [53] Steiger R H, Jäger E. Subcommission on geochronology: convention on the use of decay constants in geochronology and cosmochronology[J]. *Earth Planet. Sci. Lett.*, 1977, 36: 359–362.
- [54] Lugmair G W, Hart K. Lunar initial  $^{143}\text{Nd}/^{144}\text{Nd}$ : differential evolution of the lunar crust and mantle[J]. *Earth Planet. Sci. Lett.*, 1978, 39: 349–357.
- [55] Gill J. Orogenic Andesites and Plate Tectonics[J]. Berlin: Springer–Verlag, 1981.
- [56] Sun S S. Lead isotopic study of young volcanic rocks from mid-ocean ridges, ocean islands and island arcs[J]. *Phil. R. Soc. Lond.*, 1980, 297: 409–445.
- [57] Wilson M. Igneous Petrogenesis: A Global Tectonic Approach[M]. London: Unwin Hyman, 1989: 466.
- [58] Pitcher W S, Cobbing E J. Phanerozoic plutonism in the Peruvian edge[C]//Pitcher et al.(eds.). *Magmatism at a plate edge*, London: Blackie, 1985: 19–25.
- [59] Zindler A, Hart S R. Chemical geodynamics[J]. *Annual Review of Earth Planetary Science*, 1986, 14: 493–571.
- [60] Chen J F, Zhou T X, Xie Z, et al. Formation of positive  $\varepsilon_{\text{Nd}}$ (T) granitoids from the Alataw Mountains, Xinjiang, China, by mixing and fractional crystallization: implication for Phanerozoic crustal growth[J]. *Tectonophysics*, 2000, 328: 53–67.
- [61] Hu A Q, Jahn B M, Zhang G X, et al. Crustal evolution and Phanerozoic crustal growth in northern Xinjiang: Nd isotopic evidence. Part I. Isotopic characteristics of basement rocks[J]. *Tectonophysics*, 2000, 328: 15–51.
- [62] 王作勋, 邬继易, 吕喜朝, 等. 天山多旋回构造演化与成矿[M]. 北京: 科学出版社, 1990: 1–217.
- Wang Zuoxun, Wu Jiayi, Lv Xichao, et al. Polycyclic Tectonic Evolution and Metallogeny of the Tianshan Mountains[M]. Beijing: Science Press, 1990: 1–217 (in Chinese with English abstract).
- [63] 肖序常, 汤耀庆, 李锦铁, 等. 新疆北部及邻区大地构造[M]. 北京: 地质出版社, 1992: 1–169.
- Xiao Xuchang, Tang Yaoqing, Li Jinyi, et al. *Tectonic Evolution of Northern Xinjiang and Its Adjacent Regions*[M]. Beijing: Geological Publishing House, 1992: 1–169 (in Chinese with English abstract).
- [64] Liu Y. Early Carboniferous Radiolarian Fauna from Heiyingshan, south of the Tianshan Mountains and its geotectonic significance[J]. *Acta Geologica Sinica*, 2001, 75(1): 101–108.
- [65] 高俊, 龙灵利, 钱青, 等. 南天山: 晚古生代还是三叠纪碰撞造山带? [J]. *岩石学报*, 2006, 22(5): 1049–1061.
- Gao Jun, Long Lingli, Qian Qing, et al. South Tianshan: a Late Paleozoic or a Triassic orogen? [J]. *Acta Petrologica Sinica*, 2006, 22(5): 1049–1061.
- [66] 徐学义, 李向民, 马中平, 等. 北天山巴音沟蛇绿岩形成于早石炭世: 来自辉长岩 LA-ICPMS 锆石 U-Pb 年龄的证据[J]. *地质学报*, 2006, 80(8): 1168–1176.
- Xu Xueyi, Li Xiangmin, Ma Zhongping, et al. LA-ICPMS zircon U–Pb dating of gabbro from the Bayingou ophiolite in the northern Tianshan mountains[J]. *Acta Geologica Sinica*, 2006, 80(8): 1165–1176 (in Chinese with English abstract).
- [67] 徐学义, 夏林圻, 马中平, 等. 北天山巴音沟蛇绿岩斜长花岗岩 SHRIMP 锆石 U-Pb 年龄及蛇绿岩成因研究[J]. *岩石学报*, 2006, 22(1): 83–94.
- Xu Xueyi, Xia Linqi, Ma Zhongping, et al. SHRIMP zircon U–Pb geochronology of the plagiogranites from Bayingou ophiolite in North Tianshan Mountains and the petrogenesis of the ophiolite[J]. *Acta Petrologica Sinica*, 2006, 22(1): 83–94 (in Chinese with English abstract).
- [68] 李华芹, 周肃, 蔡红. 新疆北部尼勒克铜矿成矿作用年代学研究[J]. *地球学报*, 1997, 18(sup.): 185–187.
- Li Huaqin, Zhou Su, Cai Hong. Chronology of mineralization of the Nileke copper deposit in Northern Xinjiang[J]. *Acta Geoscientica Sinica*, 1997, 18(sup.): 185–187 (in Chinese with English abstract).
- [69] 吴明仁, 楼法生, 宋志瑞, 等. 西天山塔尔得套地区乌郎组地球化学特征和构造环境[J]. *东华理工学院学报*, 2006, 29(3): 217–224.
- Wu Mingren, Lou Fasheng, Song Zhirui, et al. Tectonic setting and geochemistry of the Wulang formation in Taerdetao, west Tianshan[J]. *Journal of East China Institute of Technology*, 2006, 29(3): 217–224 (in Chinese with English abstract).
- [70] 潘明臣, 于海峰, 梁有为, 等. 新疆吾拉斯台一带下二叠统乌郎组火山岩地球化学特征[J]. *地质与资源*, 2011, 20(6): 452–457.
- Pan Mingchen, Yu Haifeng, Liang Youwei, et al. Geochemistry of volcanic rocks of the lower Permian Wuling formation in Wulasitai area, Xinjiang[J]. *Geology and Resources*, 2011, 20(6): 452–457 (in Chinese with English abstract).
- [71] 朱志新, 董连慧, 刘淑聪, 等. 新疆西天山伊犁地块晚古生代火

- 山岩地质特征及构造意义[J]. 新疆地质, 2012, 30(3): 258–263.  
 Zhu Zhixin, Dong Lianhui, Liu Shucong, et al. Volcanic rock geological characteristics and tectonic significance of the late Paleozoic Yili block in the western Tianshan, Xinjiang[J]. Xinjiang Geology, 2012, 30(3): 258–263 (in Chinese with English abstract).
- [72] 赵军, 张作衡, 张贺, 等. 新疆阿吾拉勒山西段下二叠统陆相火山岩岩石地球化学特征、成因及构造背景[J]. 地质学报, 2013, 87(4): 525–541.  
 Zhao Jun, Zhang Zuoheng, Zhang He, et al. Geochemistry, petrogenesis and tectonic setting of the lower Permian series volcanic rocks from western Awulale mountain, Xinjiang[J]. Acta Geologica Sinica, 2013, 87(4): 525–541 (in Chinese with English abstract).
- [73] 尹永红. 西天山群吉萨依铜矿床形成背景与成矿特征研究[D]. 中国地质大学(北京), 2013:1–83.  
 Yan Yonghong. Study on the Forming Background and the
- Mineralization Characteristics Reseach of the Qunjisayi Copper Deposit, Wester Tianshan[D]. Beijing: China University of Geoscience, 2013:1–83 (in Chinese with English abstract).
- [74] 王玉往, 王京彬, 龙灵利, 等. 新疆北部大地构造演化阶段与斑岩–浅成低温热液矿床的构造环境类型[J]. 中国地质, 2012, 39(3): 695–716.  
 Wang Yuwang, Wang Jingbin, Long Lingli, et al. Tectonic evolution stages of northern Xinjiang and tectonic types of porphyry–epithermal deposits[J]. Geology in China, 2012, 39(3): 695–716 (in Chinese with English abstract).
- [75] 钱青, 王岳明, 李惠民, 等. 甘肃老虎山闪长岩的地球化学特征及其成因[J]. 岩石学报, 1998, 14(4): 520–528.  
 Qian Qing, Wang Yueming, Li Huimin, et al. Geochemical characteristics and genesis of diorites from Laohushan, Gansu Province[J]. Acta Petrologica Sinica, 1998, 14(4): 520–528 (in Chinese with English abstract).

## Geochemistry and zircon U–Pb geochronology of the diorite associated with the Wuling iron deposit in Western Tianshan Mountains, Xinjiang

DUAN Shi-gang<sup>1,2</sup>, ZHANG Zuo-heng<sup>2</sup>, WEI Meng-yuan<sup>3</sup>, TIAN Jing-quan<sup>3</sup>,  
 JIANG Zong-sheng<sup>2</sup>, LI Feng-ming<sup>4</sup>, ZHAO Jun<sup>1</sup>, WANG Hou-fang<sup>3</sup>

(1. College of Earth Science and Land Resources, Chang'an University, Xi'an 710054, Shaanxi, China; 2. MLR Key Laboratory of Metallogeny and Mineral Assessment, Institute of Mineral Resources, Chinese Academy of Geological Sciences, Beijing 100037, China; 3. No. 3 Geological Party, Xinjiang Bureau of Geology and Mineral Resources, Korla 841000, Xinjiang, China;  
 4. Xinjiang Bureau of Geology and Mineral Resources, Urumqi 830000, Xinjiang, China)

**Abstract:** The Wuling diorite stock was intruded in volcanoclastic rocks of the Carboniferous Dahalajunshan Formation. Iron ore deposits were discovered in the contact zone or the interior of the stock. Zircon LA-ICP-MS U-Pb dating of the diorite yielded a weighted mean  $^{206}\text{Pb}/^{238}\text{U}$  age of  $(307.7 \pm 0.8)\text{ Ma}$ . Positive  $\varepsilon_{\text{Nd}}(\text{t})$  values vary from 3.1 to 4.6, initial  $^{87}\text{Sr}/^{86}\text{Sr}$  ratios are relatively low (0.7043–0.7046), and Nd model ages vary between 695Ma and 818Ma and fall on the mantle trend line in the  $^{87}\text{Sr}/^{86}\text{Sr}(\text{t})$  versus  $\varepsilon_{\text{Nd}}(\text{t})$  diagram. These data indicate a mantle source for the Wuling diorite. However, high Th values ( $1.61\text{--}3.24\mu\text{g/g}$ ) and Th/Ta ratios (6.1–7.9) imply that the magma experienced a certain degree of contamination by continental crust. Therefore, the Wuling diorite magma might have been formed by the fractional crystallization of basaltic magma affected by crustal material. Although some traces of arc magmatism can be detected, the Wuling diroite was actually formed by intraplate magmatism. This diorite was emplaced when block rotation occurred between the Yili and Tarim plates after the termination of the West Tianshan accretionary orogeny. It is inferred that the generation of the magma was probably related to the detachment of an orogenic root zone or a local squeezing–stretching structural transition zone within the Yili plate.

**Key words:** marine volcanogenic iron deposit; zircon U–Pb dating; Sr–Nd isotopes; Wuling; Awulale; Western Tianshan Mountains

**About the first author:** DUAN Shi-gang, male, born in 1983, doctor, assistant researcher, engages in the study of geology and geochemistry of ore deposits; E-mail: dsg1102231@163.com.